

## Leaf Liquid Extract of Citrus X-Latifolia for Corrosion Inhibition of Structural Steel AISI 1045 in Acidic Environment

Juan Carlos Trinidad González\*, Héctor Herrera Hernández, Araceli Mandujano Ruiz, José Guadalupe Miranda Hernández

Universidad Autónoma del Estado de México, Laboratorio de Investigación en Electroquímica y Corrosión de Materiales Industriales. Blvd. Universitario s/n, Predio San Javier Atizapán de Zaragoza, Estado de México, 54500, México.

\*Corresponding author: Juan Carlos Trinidad González, email: [carlos.trini.ct@gmail.com](mailto:carlos.trini.ct@gmail.com)

Received March 29<sup>th</sup>, 2023; Accepted July 5<sup>th</sup>, 2023.

DOI: <http://dx.doi.org/10.29356/jmcs.v67i4.2029>

*We want to express our utmost respect and gratitude to the emeritus SNI researchers who have contributed significantly to the field of electrochemistry in Mexico. Dr. Yunny Meas Vong, Dr. Joan Genescá Llongueras, Dr. Ignacio González Martínez, Dr. Jorge Ibañez Cornejo, Dr. Omar Solorza Feria, and Dr. Elsa Miriam Arce Estrada have worked tirelessly and with a scientific passion for promoting new knowledge that benefits our environment and society. Their legacy serves as an inspiration to future researchers in the noble field of electrochemistry, as well as to us.*

**Abstract.** In the present research work, the corrosion inhibition capacity of a liquid extract based on *Citrus X-Latifolia* leaves was evaluated as a **green inhibitor** that complies with a natural, economical, and environmentally friendly option. The tests were carried out on a carbon steel AISI 1045 exposed to an acid corrosive medium of 10 mL H<sub>2</sub>SO<sub>4</sub> (0.5 M) to which various concentrations of the extract were dosed as follows: 40, 80, 120, 160, 200, 240, 280, 320, 360 and 400 ppm under standard conditions. Characterization by FT-IR was carried out to detect functional groups of the extract. The inhibitory behavior was recorded by electrochemical techniques (Tafel polarization and EIS). Finally, optical microscopy was used to evaluate the corrosion morphology. The results reveal that the adsorption of the extract molecules on steel follows the behavior of a Langmuir isotherm, reaching a maximum efficiency of 89 % with a concentration of 400 ppm. Finally, an evident change in the surface morphology of the steel sample is observed, thus reducing the pitting corrosion attack on AISI 1045 steel.

**Keywords:** Industrial steels; *Citrus X-Latifolia* liquid extract; green inhibitor; Electrochemical Impedance Spectroscopy EIS; Tafel polarization.

**Resumen.** En el presente trabajo de investigación se evaluó la capacidad de inhibición de la corrosión de un extracto líquido a base de hojas de *Citrus X-Latifolia* como inhibidor verde que cumpla como una opción natural, económica y amigable con el medio ambiente. Los ensayos se realizaron sobre un acero al carbono AISI 1045 expuesto a un medio ácido corrosivo de 10 mL de H<sub>2</sub>SO<sub>4</sub> (0,5 M) al que se dosificaron diversas concentraciones del extracto: 40, 80, 120, 160, 200, 240, 280, 320, 360 y 400 ppm en condiciones estándar. Se realizó una caracterización por FT-IR para detectar los grupos funcionales del extracto. El comportamiento inhibitorio se registró mediante técnicas electroquímicas (polarización de Tafel y EIS). Finalmente, se utilizó microscopía óptica para evaluar la morfología de la corrosión. Los resultados revelan que la adsorción de las moléculas del extracto sobre el acero sigue el comportamiento de una isoterma de Langmuir, alcanzando una eficiencia máxima del 89 % con una concentración de 400 ppm. Finalmente, se observa un cambio evidente en la morfología

superficial de la muestra de acero, reduciéndose así el ataque de corrosión por picaduras en el acero al carbono 1045.

**Palabras clave:** Aceros industriales; extracto líquido de *Citrus X-Latifolia*; inhibidor ecológico; Espectroscopía de impedancia electroquímica (EIS); polarización de Tafel.

---

## Introduction

Steel is a crucial industrial material used for many years ago to manufacture pipes, machinery, structures, and tools; unfortunately, its degradation occurs due to corrosion, a significant problem that generates costly economic losses and irreversible damage [1]. Therefore, preventing and controlling this phenomenon is essential when developing a monitoring or maintenance plan. A promising solution to mitigate corrosion is using **green inhibitors** [2, 3]; these innovative inhibitors contain organic molecules extracted from organic plants, leaves, or fruits that suppress oxidation-reduction reactions when steel is exposed to aggressive environments such as acidic media. Depending on the type of metal-media interaction, green inhibitors can generate protective layers (thin film inhibitors) or work through an adsorption process, in which a charge transfer occurs between the inhibitor and the metal surface, forming a protective layer that prevents contact with the metal, in addition, they offer essential economic advantages, as they are relatively inexpensive and environmentally friendly [4-6]. Organic plant extracts contain phytochemical compounds, including heteroatoms such as sulfur, phosphorus, nitrogen, and oxygen, which effectively prevent metal corrosion; these heteroatoms act as adsorption centers, allowing easy adsorption on the metal surface. Several plant and fruit extracts have been studied, showing a high inhibition efficiency in different corrosive environments reaching inhibition efficiency of 80 to 96 %; some of them are *Morinda Citrifolia* leaves, *Aloe vera* gel, *Opuntia Ficus*, *Pomegranate*, among others [7-11].

The *Citrus X-Latifolia* plant (known as **Persian lemon**) is cultivated around the world, and Mexico is one of the leading exporters of this fruit; it belongs to the *Rutaceae* family along with the *Citrus X-aurantifolia* plant of which studies have been conducted to evaluate and characterize the corrosion inhibition capabilities in carbon steels in acid medium from the extract prepared with its leaves, according to Rajesh H. et al. [12] found efficiencies (IE) higher than 90% using low concentrations of the extract. At the same time, Rifat Mohammed Dakhil R.M. et al. [13] reported that efficiencies of 80 % are maintained with increasing temperature; therefore, it is of great interest to evaluate the leaves of *Citrus X-Latifolia* as a possible corrosion inhibitor for AISI 1045 steel exposed in an acidic medium H<sub>2</sub>SO<sub>4</sub> (0.5 M) under standard conditions and implementing the use of electrochemical characterization techniques such as Electrochemical Impedance Spectroscopy (EIS) and Potentiodynamic Polarization (Tafel) to determine the corrosion rate ( $V_{\text{corr}}$ ) generated when different concentrations of this extract are added.

Another reason for considering using the leaves of the *Citrus X-Latifolia* plant instead of its fruits is that the leaves are often discarded, leading to waste accumulation and environmental pollution, thus representing an opportunity to explore alternative uses for this resource, particularly in the corrosion of materials.

## Experimental

### Preparation of extract and acid.

The leaves of *Citrus X-Latifolia* were collected, washed with soap, and rinsed with distilled water to be later dehydrated naturally, taking advantage of sunlight (this process lasted about three months), once dried they were crushed in a mortar until obtaining fine particles that were weighed on a balance until getting 50 gr of powder that was poured into a flask and filled with 500 ml of ethanol; finally, this solution was macerated for two weeks before being used in the tests. The concentrations in ppm of the *Citrus X-Latifolia* extract used

were: 40, 80, 120, 160, 200, 240, 280, 320, 360, and 400, this process is shown in Fig. 1 [7, 13]. For the corrosive medium, a solution of  $\text{H}_2\text{SO}_4$  (0.5 M) was prepared from concentrated acid and distilled water.

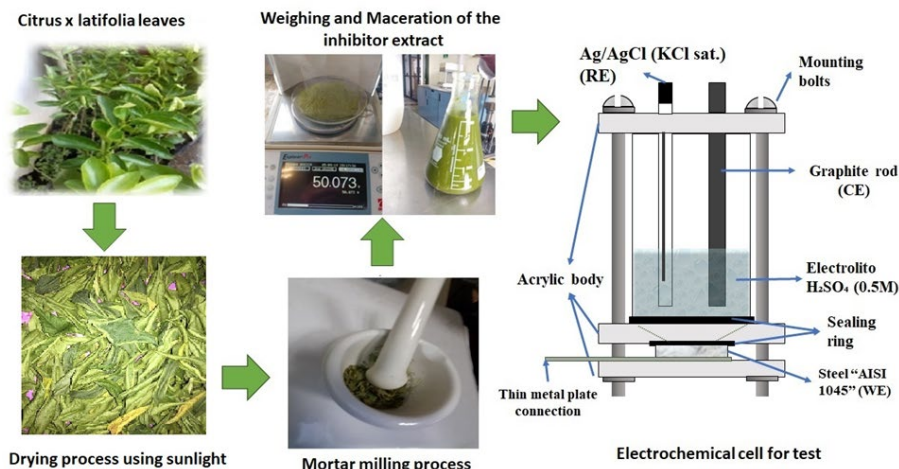


**Fig. 1.** Preparation of *Citrus X-Latifolia* leaf liquid extract and Electrochemical cell for tests.

### Specimens preparation

For AISI 1045 steel specimens, cylindrical bar coupons were cut and shaped into samples 2.5 cm in diameter and 1 cm in width; the chemical composition of this steel is Si 0.22 %, Mn 0.75 %, S 0.50 %, P 0.40 %, C 0.40-0.50%, and balance Fe. The samples were then abraded using different sizes of silicon carbide paper with the numbers: #80, #240, #300, #400, #600, and #1200 until achieving a mirror finish with an alumina cloth. After polishing, the samples were washed with water, soap, and acetone and dried with hot air. Finally, the specimens were kept in a desiccator for testing.

### Electrochemical evaluation

For corrosion test, acrylic cells were manufactured on a milling machine (a particular cell designed by DR.3H) [7, 9], to which 10 mL of  $\text{H}_2\text{SO}_4$  (0.5 M) were added. The cell has a configuration of 3 electrodes: 2 are connected at the top, the reference electrode (RE) of Ag/AgCl (KCl sat.), and a graphite bar as the counter electrode (CE), while at the bottom steel is found below as a working electrode (WE) [14], this assembly can be seen in Fig. 1. A Parstat 4000 potentiostat/galvanostat from Prince Applied Research® (serial number 14181860) linked to a PC and controlled by Versa Studio software for acquisition data was used for experimentation. The sequence described in Fig. 2 begins with the test of the steel exposed to acid, applying open circuit potential (OCP) for 1 hour to monitor the equilibrium potential of the system, later EIS technique is used with a sweep of frequencies ranging from 100KHz at 10mHz, with an amplitude of 10 mV with 10 points/decade, at the end Tafel was applied, with a sweep potential of  $\pm 250$  mV, and a sweep speed of 1.66 mV/s [15-17]. Once this first sequence of tests was finished, the first extract concentration of 40 ppm was added, and the OCP, EIS, and Tafel techniques were applied again. This process will be repeated by adding each dosage within the same test.

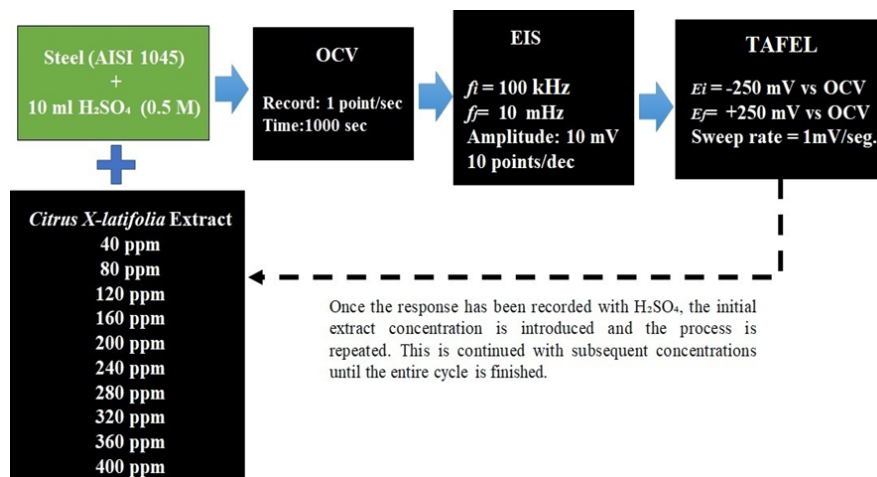


**Fig. 2.** Experimental sequence for testing Liquid Extract of *Citrus X-Latifolia* leaf on AISI 1045.

### Metallic surface and extract characterization

Functional groups present in the *Citrus X-Latifolia* extract were analyzed using FT-IR infrared spectroscopy; for this purpose, a Perkin Elmer Spectrum 100 FTIR unit, equipped with a universal ATR sampling accessory and applying a wave number of 400-4000  $\text{cm}^{-1}$ . Metallographic images were taken to assess the impact of the inhibitor extract on the steel surface using an OLYMPUS brand Inverted Metallurgical Microscope GX51; the captures correspond to different stages, the initial state of the steel, after exposure to  $\text{H}_2\text{SO}_4$  (0.5 M), and after tests with inhibitor extract.

## Results and discussion

### FT-IR results

The FT-IR spectrum obtained from the *Citrus X-Latifolia* extract is shown in Fig. 3; 5 signals are detected: a peak located at 3323  $\text{cm}^{-1}$  identified as the presence of an OH group, at 2926  $\text{cm}^{-1}$  related with the stretching vibration (asymmetric) of the C-H group, the peak located at 1608  $\text{cm}^{-1}$  is related to an H-O-H group, the 1724  $\text{cm}^{-1}$  peak is characteristic of a carboxylic functional group (-COOH), finally, in the peak located at 1039  $\text{cm}^{-1}$  related to the stretching vibration of the C-O bond attributed to carbohydrates (sugars and starch). These functional groups contain heteroatoms (P, O, S, N), which have an electron density that promotes their adsorption on the steel surface through coordinated bonds.

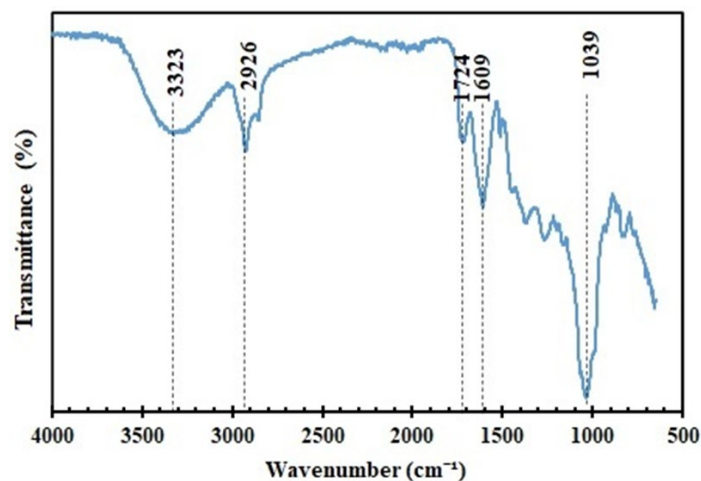


**Fig. 3.** FT-IR spectra of *Citrus X-Latifolia* extract.

### Potentiodynamic polarization curves (TAFEL)

The results of the potentiodynamic polarization curves are shown in Fig. 4; it can be observed a marked change in the corrosion potential ( $E_{corr}$ ) between the anodic curve of the steel in 0.5 M  $H_2SO_4$  (Blank) concerning the curves generated from the concentrations of the inhibitor extract, it is also noted a change in the shape of the anodic slope related to a decrease in the exchange current density ( $J_o$ ) when the inhibitor is added. The shift of the potential towards more positive values (nobler) and the shape of the curves with the inhibitor comply with the behaviour of an anodic type inhibitor, according to Sastri S.V. [4], this type of inhibitor forms a film that adsorbs on the surface of the steel, preventing its dissolution.

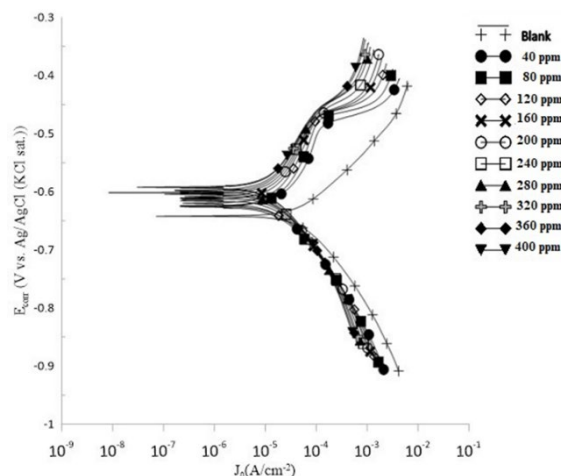


**Fig. 4.** Potentiodynamic polarization curves for AISI 1045 in  $H_2SO_4$  (Blank) and *Citrus X-Latifolia* Inhibitor.

The anodic ( $b_a$ ) and cathodic ( $b_c$ ) Tafel slopes of the polarization curves with blank and inhibitor concentrations were calculated using the EC-Lab software by Bio-Logic®. The obtained values were substituted into the Stern-Geary expression (equation 1) to get the Polarization Resistance ( $R_p$ ) and corrosion rate ( $V_{corr}$ ); the results are summarized in Table 1.

$$I_{\text{corr}} = \frac{b_a b_c}{2.303 (b_a + b_c)} \left( \frac{1}{R_p} \right) \quad (1)$$

Table 1 shows the results of the potentiodynamic polarization technique; in general, a decrease in the potential and the corrosion current is observed as each of the concentrations of *Citrus X-Latifolia* extract is added; on the other hand, these current values promote a better corrosion rate of 0.19 mm/year with a concentration of 360 ppm.

**Table 1.** Potentiodynamic polarization results for different doses of *Citrus X-Latifolia* extract in H<sub>2</sub>SO<sub>4</sub> (0.5 M).

| Inhibitor concentration (ppm) | $E_{\text{corr}}$ (V vs. Ag/AgCl KCl sat.) | $i_{\text{corr}}$ (A/cm <sup>2</sup> ) | $V_{\text{corr}}$ (mm/y) | IE%   |
|-------------------------------|--|--|--------------------------|-------|
| Blank                         | -0.640                                     | $1.55 \times 10^{-5}$                  | 0.174                    | -     |
| 40                            | -0.622                                     | $4.38 \times 10^{-6}$                  | 0.049                    | 71.83 |
| 80                            | -0.623                                     | $3.83 \times 10^{-6}$                  | 0.043                    | 75.36 |
| 120                           | -0.617                                     | $3.07 \times 10^{-6}$                  | 0.034                    | 80.27 |
| 160                           | -0.612                                     | $3.31 \times 10^{-6}$                  | 0.037                    | 78.72 |
| 200                           | -0.608                                     | $2.82 \times 10^{-6}$                  | 0.032                    | 81.84 |
| 240                           | -0.603                                     | $3.02 \times 10^{-6}$                  | 0.034                    | 80.56 |
| 280                           | -0.599                                     | $2.56 \times 10^{-6}$                  | 0.029                    | 83.54 |
| 320                           | -0.598                                     | $2.26 \times 10^{-6}$                  | 0.025                    | 85.43 |
| 360                           | -0.592                                     | $1.69 \times 10^{-6}$                  | 0.019                    | 89.14 |
| 400                           | -0.590                                     | $2.15 \times 10^{-6}$                  | 0.024                    | 86.16 |

### Electrochemical impedance spectroscopy (EIS)

The resistive behavior of AISI 1045 steel exposed to 0.5 M H<sub>2</sub>SO<sub>4</sub> and various concentrations of *Citrus X-Latifolia* extract was recorded using the EIS technique. Fig. 5 shows the Nyquist diagrams ( $Z_{re}$  VS  $Z_{im}$ ), which present a semicircular shape whose size increases as the inhibitor concentrations are added, indicating a remarkable increase in the resistance to  $R_{ct}$  charge transfer between the steel in acid and as the inhibitor concentrations are added.

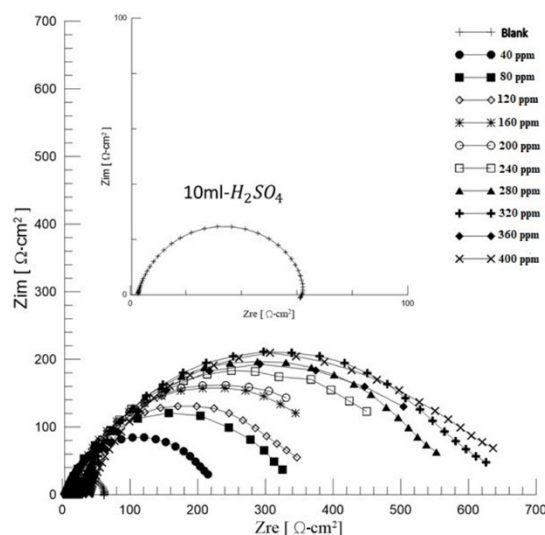


**Fig. 5.** Nyquist plots corresponding to AISI 1045 in H<sub>2</sub>SO<sub>4</sub> (Blank) and the results of *Citrus X-Latifolia* extract.

To calculate the electrical parameters of EIS, the Nyquist diagrams were adjusted using an equivalent electrical circuit (EEC) using Zsim® software. Fig. 6(a) shows the fit of the AISI 1045 steel in H<sub>2</sub>SO<sub>4</sub>; the EEC fitted to the semicircle shape was a Randles type [18] and consisted of two resistors; the solution resistance ( $R_{sol}$ ), the charge transfer resistance  $R_{ct}$  and a constant phase element (CPE) which replaces the electrochemical double layer capacitance ( $C_{dl}$ ) and is expressed in units of  $\mu\text{F}$ ; the estimation of  $C_{dl}$  is carried out employing expression 2, this model is used to simulate the physical-chemical processes analogously when a metal is in contact with a corrosive medium; however, when adding the inhibitor the Randles model does not generate a good fit, so a different circuit was proposed which is shown in Fig. 6(b) where the modification of the EEC can be seen by integrating three resistors: solution Resistance ( $R_{sol}$ ), inhibitor Charge transfer Resistance ( $R_{inh}$ ) and Steel Charge Transfer Resistance ( $R_{ct}$ ), as well as two CPE constant phase elements.

$$C_{dl} = \text{CPE} \cdot \omega_{\theta_{\max}}^{(a-1)} \quad (2)$$

Where:  $\omega_{\theta_{\max}}$  is the maximum frequency in the Nyquist semicircle, and the exponent  $a$  is a constant obtained by fitting and whose values range from 0.5 ~ 0.9. [18, 19]

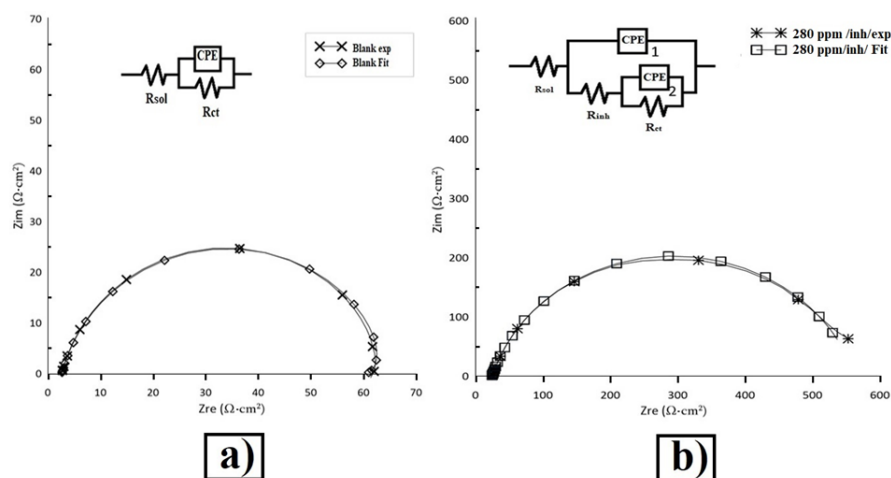


**Fig. 6.** Fitted Nyquist diagrams and equivalent electrical circuit (EEC) representation corresponding to (a) AISI 1045 in H<sub>2</sub>SO<sub>4</sub> (0.5 M), (b) AISI 1045 in H<sub>2</sub>SO<sub>4</sub> (0.5 M) + *Citrus X-Latifolia* leaf extract, example of 14 mL added.

The results reported in Table 2 show the values for  $R_{sol}$ ,  $R_{ct}$ ,  $C_{dl}$ , and finally the efficiency in percentage IE. It can be observed that the addition of 40 ppm of the inhibitor generates an increase in  $R_{ct}$ , as well as an increase in capacitance, which suggests that the exchange of electrons between the medium and the steel decreases due to the formation of an insulating barrier on the surface of the metal, however, according to study from Bryan H. et al. [20], which suggests that the thickness of the film formed is related to the capacitance value, so that the higher the value of  $C_{dl}$ , the lower its thickness, which implies that the thickness created by the *Citrus X-Latifolia* extract is not large and continues to permeate the corrosive ions of the medium in smaller quantities.

**Table 2.** Corrosion parameters obtained from Electrochemical Impedance Spectroscopy.

| Inhibitor concentration (ppm) | $i_{corr}$ (A/cm <sup>2</sup> ) | $R_{sol}$ (Ω·cm <sup>2</sup> ) | $R_{ct}$ (Ω·cm <sup>2</sup> ) | $C_{dl}$ (μF/cm <sup>2</sup> ) | IE%   |
|-------------------------------|---------------------------------|--------------------------------|-------------------------------|--------------------------------|-------|
| Blank                         | $4.23 \times 10^{-5}$           | 2.63                           | 320.18                        | 238.27                         | -     |
| 40                            | $5.83 \times 10^{-6}$           | 3.31                           | 1140.07                       | 586.00                         | 71.92 |

|     |                       |       |         |         |       |
|-----|-----------------------|-------|---------|---------|-------|
| 80  | $8.26 \times 10^{-6}$ | 6.30  | 1662.98 | 805.11  | 80.75 |
| 120 | $7.10 \times 10^{-6}$ | 9.21  | 1760.32 | 897.33  | 81.81 |
| 160 | $6.81 \times 10^{-6}$ | 12.31 | 2092.87 | 957.31  | 84.70 |
| 200 | $5.99 \times 10^{-6}$ | 15.17 | 2157.93 | 966.03  | 85.16 |
| 240 | $5.78 \times 10^{-6}$ | 20.02 | 2508.26 | 981.51  | 87.23 |
| 280 | $4.84 \times 10^{-6}$ | 24.07 | 2731.06 | 1077.80 | 88.28 |
| 320 | $4.01 \times 10^{-6}$ | 28.60 | 2980.51 | 1064.75 | 89.26 |
| 360 | $3.20 \times 10^{-6}$ | 34.54 | 2942.40 | 1205.00 | 89.12 |
| 400 | $4.01 \times 10^{-6}$ | 39.26 | 3008.73 | 1066.85 | 89.36 |

Fig. 7 presents the corrosion rates for both the Tafel and EIS techniques. The results reveal a substantial decrease in  $V_{corr}$  for the steel sample when exposed to *Citrus X-Latifolia* doses compared to a blank sample. The lowest  $V_{corr}$  values were obtained at a concentration of 360 ppm, with Tafel showing 0.019 mm/year and EIS showing 0.035 mm/year. Overall, the results obtained from both techniques are very similar, indicating a strong correlation between Tafel and EIS.

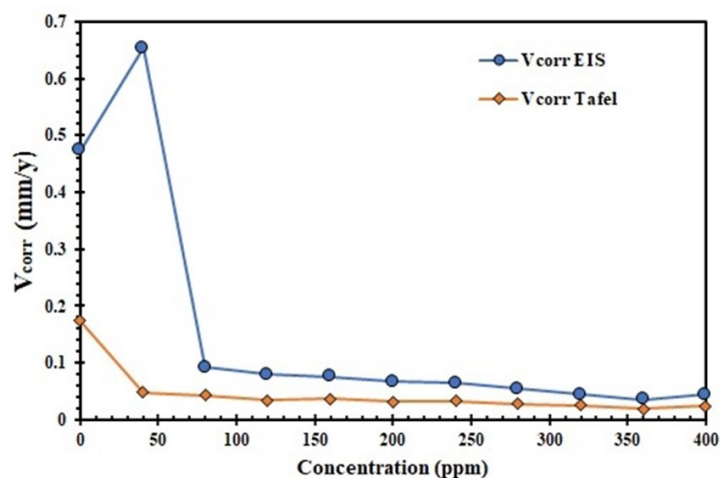


**Fig. 7.** Corrosion rate behaviour obtained by Tafel and EIS techniques of *Citrus X-Latifolia* inhibitor extract dosed in  $H_2SO_4$  (0.5 M) at 25 °C.

### Inhibitor efficiency

Corrosion Inhibition Efficiency (IE) can be calculated using the coverage degree " $\theta$ " which represents the value of the covered metal surface from the inhibitor extract, the equations used in this investigation are shown below:

$$\theta = \frac{i_{corr}(\text{Blank}) - i_{corr}(\text{inhibitor})}{i_{corr}(\text{Blank})} \quad (3)$$

$$\theta = \frac{\frac{1}{R_{ct}}(\text{Blank}) - \frac{1}{R_{ct}}(\text{inhibitor})}{\frac{1}{R_{ct}}(\text{Blank})} \quad (4)$$

$$IE(\%) = \theta \times 100 \quad (5)$$

Where  $i_{corr}$  is the corrosion current obtained from Tafel, and  $R_{ct}$  is the charge transfer resistance obtained from EIS, using equations 3 or 4, the value of  $IE$  (%) can be calculated easily with expression 5 [12, 21]. Fig. 8 shows that the efficiency of the inhibitor was very promising, from 120 ppm with 80 % IE from both techniques and reaching 89 % IE at the final concentration of 320 ppm.

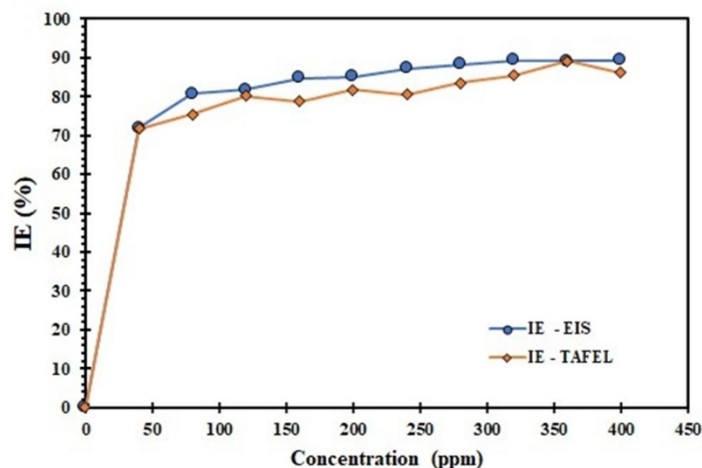


**Fig. 8.** Efficiency percentages (IE) obtained by Tafel and EIS techniques for the added volumes of *Citrus X-Latifolia* extract in  $H_2SO_4$  (0.5 M) at 25 °C.

### Adsorption mechanism

The modeling of adsorption isotherms is beneficial in providing information on the ability of the organic molecule of the inhibitor to concentrate on the metal surface. There are two adsorption mechanisms: physical adsorption (physisorption) and chemical adsorption (chemisorption). The physisorption is carried out by interactions of Van Der Waals forces between the active sites of the metal surface; such adsorbed molecules require energy values below -20 kJ/mol to form multilayers. While the chemisorption process, the interactions involve charge exchange and analogous force-coordinated bonding between the metal surface and the adsorbed molecules. Between the metal surface and the organic molecules, this monolayer formation requires energies above -40 KJ/mol.[7, 22-25]

With equations 3 or 4, it is possible to perform the calculation for different adsorption models; the most used in the literature is the Langmuir model, which is calculated using the following expression:

$$\frac{C}{\theta} = \frac{1}{k_{ads}} + C \quad (6)$$

where  $C$  is the concentration of the inhibitors in the bulk electrolyte,  $K_{ads}$  is the adsorption equilibrium constant.

In Fig. 9, equation 6 can be interpreted as an equation of the straight line; which shows that the behavior of *Citrus X-Latifolia* extract tends to be linear, and the correlation coefficient approaches 1; using the slope value, the Gibbs adsorption free energy ( $\Delta G^{\circ}_{ads}$ ) can be estimated by 7:

$$\Delta G^{\circ}_{ads} = -RT \ln K_{ads} \quad (7)$$

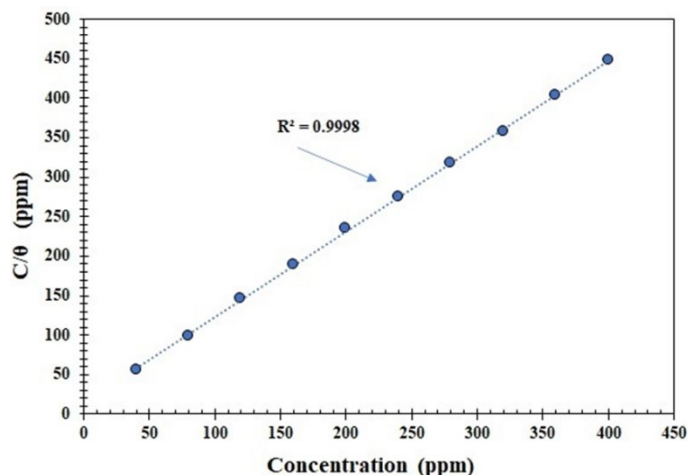


**Fig. 9.** Langmuir Isotherm representation for adsorption of *Citrus X-Latifolia* on AISI 1045 Surface exposes in 0.5 M H<sub>2</sub>SO<sub>4</sub> at 25 °C.

Thermodynamic results obtained from analyzing the Langmuir isotherm's linear fit are presented in Table 3. The negative Gibbs energy ( $\Delta G^{\circ}_{ads}$ ) value (-3.04 kJ/mol) indicates that the *Citrus x Latifolia* extract undergoes spontaneous adsorption on the AISI 1045 metal surface through a physisorption process. This behavior is similar to other organic molecules like *Lime Juice*, *Opuntia Ficus Indica* extract or synthetic inhibitors such as pantoprazole used in hydrocarbon pipelines [26-29].

**Table 3.** Isothermal parameters results of *Citrus X-Latifolia* leaf extract on AISI 1045 surface in H<sub>2</sub>SO<sub>4</sub> at 25 °C.

| Isotherm | Intercept | Slope | $K_{ads}$ | $R^2$ | $\Delta G_{ads}$<br>(kJ·mol <sup>-1</sup> ) |
|----------|-----------|-------|-----------|-------|---|
| Langmuir | 14.53     | 1.08  | 0.06      | 0.99  | -3.04                                       |

The attack on the surface of the steel after the experimentation was recorded in Fig. 10, where the polished steel before the electrochemical tests is shown (Fig. 10(a)); after the exposure with 0.5 M H<sub>2</sub>SO<sub>4</sub>, the presence of pitting is observed, including the formation of oxide residues on the surface (Fig. 10(b)); finally, it can be observed in Fig. 10(c) that *Citrus X-Latifolia* extract obtained good results changing the type of corrosion since the inhibitor molecules obey an adsorption mechanism thus forming an organic barrier on the surface of the steel, corresponding to a decrease in the corrosion rate.

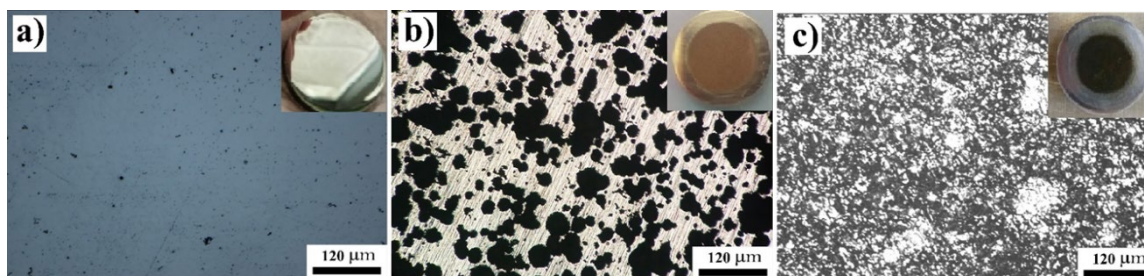


**Fig. 10.** Metallographic of AISI 1045 steel in (a) initial state before attack, (b) attacked by H<sub>2</sub>SO<sub>4</sub>, and (c) after *Citrus X-Latifolia* extract exposition.

## Conclusions

The extract prepared from *Citrus X-Latifolia* leaves is a suitable corrosion inhibitor for AISI 1045 steel against 0.5M H<sub>2</sub>SO<sub>4</sub> solution under standard conditions. The electrochemical results using Tafel show that the behavior of this inhibitor is an anodic type and modifies the corrosion potential towards more noble values. In contrast, EIS measurements show that charge transfer resistance increases as each extract concentration is dosed, finding comparative corrosion rates for both techniques. The best efficiency observed in EIS and Tafel was 89 % under a concentration of 360 ppm. Finally, Langmuir adsorption isotherm shows that the extract uses a physical adsorption mechanism (physisorption) and creates a protective layer on the steel.

## Acknowledgements

The authors express their gratitude for the support received by the UAEM CU Valle de México University, where the development of this research was carried out, as well as to COMECyT for the financial support granted during the program "*Cátedras de Investigación 2021-2022*", which helps young researchers to perform postdoctoral stays in Academic Institutions and Research Centers in the state of Mexico. We are also grateful for the support from the National System of Researchers (*SNI - CONACyT*). Finally, DR.3H would like to express its gratitude to his father Eleazar Herrera Flores for his exceptional love, guidance, care, knowledge, and affection. He will always be remembered fondly forever.

## References

1. Rosidah, A.; Setyowati, V.; Suheni, S.; Rijayanto, R. *J. Mech. Eng. Sci. and Innov.* **2021**, 1, 49-55. DOI: <https://doi.org/10.31284/j.jmesi.2021.v1i2.2183>.
2. Ortega, R. A. T.; Barrantes, S. L. V.; Casallas, M. B. D.; Cortés, S. N. J. *DYNA*, **2021**, 88, 217, 160-168. DOI: <https://doi.org/10.15446/dyna.v88n217.93871>.
3. Sanyal, B. *Prog. Org. Coat.* **1981**, 9, 165–236. DOI: [https://doi.org/10.1016/0033-0655\(81\)80009-X](https://doi.org/10.1016/0033-0655(81)80009-X).
4. Sastri, V.S., in: *Green corrosion inhibitors*. Ed. New Jersey John Wiley & Sons, Inc. **2011**.
5. Suarez, H. R.; Gonzalez, R. J. G.; Dominguez, P. G. F.; Martínez V. A. *Anti-Corros Methods Mater.* **2014**, 61, 224-231. DOI: <https://doi.org/10.1108/ACMM-01-2013-1238>.
6. Hossain, N.; Mohammad, A. C.; Mohamed, K. *J. Adhes. Sci. Technol.* **2021**, 35, 673-690. <https://doi.org/10.1080/01694243.2020.1816793>.
7. Barreto, E. M. Centro Universitario UAEM Valle de México: Atizapán de Zaragoza, Edo. de México. 2016.
8. Hernández, H. H.; Franco, T. M. I.; Molina, A. C. A.; Miranda, H. J. G.; Orozco, C. R., in: *CONAMET/SAM*. Concepción-Chile. 2015.
9. Herrera, H. H.; Tronco, M. I. F.; Miranda, H. J. G.; Hernández, S. E.; Espinoza, V. A.; Fajardo, G. Av. *Cien. Ing.* **2015**, 6, 9-23.
10. Abboud, Y.; Tanane, O.; El Bouari, A.; Salghi, R.; Hammouti, B.; Chetouani, A.; Jodeh, S. *Corros. Eng. Sci. Technol.* **2015**, 1-9. DOI: <https://doi.org/10.1179/1743278215Y.0000000058>.
11. Rochaa, J.C. d.; Gomesa, J. A. d. C. P.; D'Elia, E. *Mater. Res.* **2014**, 17, 1581-1587. DOI: <http://dx.doi.org/10.1590/1516-1439.285014>.
12. Haldhar, R., D.; Prasad, D.; Bhardwaj, N. *J. Adhes. Sci.* **2019**, 33, 1169-1183. DOI: <https://doi.org/10.1080/01694243.2019.1585030>.
13. Dakhil, R. M.; Tayser, S. G.; Ahmed, A. A. A.; Abdul, A. H. K. *Green Chem. Lett. Rev.* **2018**, 11, 559-566. DOI: <https://doi.org/10.1080/17518253.2018.1547796>.

14. Meas, Y.; Rodríguez, F. J.; Genescá, J.; Mendoza, J.; Durán, R.; Uruchurtu, J.; Malo, J. M.; Martínez, E. A.; Arganiz, C.; Pérez, T.; Martínez, A.; Chacón, J. G.; Gaona, G.; Almeraya, F. M.; González, J. G. in: *Técnicas Electroquímicas para el Control y Estudio de la Corrosión*, Ed. UNAM, Querétaro, **2002**.
15. Unnimaya; Prakasha, S.; Preethi, K.; Sneha, K. *J. Solid State Electrochem.* **2023**, 27, 255-270. DOI: <https://doi.org/10.1007/s10008-022-05315-7>.
16. Hernández, H. H.; Franco, T. M. I.; Molina, A. C. A.; Miranda, H. J. G.; Orozco, C. R., in: *Memorias del Congreso Internacional de Investigación Académica Journals Tabasco*. Tabasco, México. **2016**.
17. Mendonça, G. L. F.; Costa, S. N.; Freire, V. N.; Casciano, P. N. S.; Correia, A. N. *Corros. Sci.* **2017**, 115, 41-55. DOI: <https://doi.org/10.1016/j.corsci.2016.11.012>.
18. Hernández, H. H.; Ruiz, R. A. M.; Trinidad, G. J. C.; González, M. C. O.; Miranda, H. J. G.; Mandujano, R. A.; Morales, H. J.; Orozco, C. R., in: *Electrochemical Impedance Spectroscopy*. Ed. IntechOpen. **2020**.
19. Magar, H.S.; Hassan, R. Y. A.; Mulchandani, A. *MDPI.* **2021**, 2, 19. DOI: <https://doi.org/10.3390/s21196578>.
20. Hirschorn, B.; Orazem, M. E.; Tribollet, B.; Vivier, V.; Frateur, I.; Musiani, M. *Electrochim. Acta.* **2010**, 55, 6218-6227. DOI: <https://doi.org/10.1016/j.electacta.2009.10.065>.
21. Kamal, C.; Sethuraman, M. G. *Arab. J. Chem.* **2012**, 5, 155-161. DOI: <https://doi.org/10.1016/j.arabj.2010.08.006>.
22. Khaled, K. F. *Appl. Surf. Sci.* **2010**, 256, 6753-6763. DOI: <https://doi.org/10.1016/j.apsusc.2010.04.085>.
23. Adah, C.A.; Adejo, S. O.; Gbertyo, J. A.; Ogwuche, A. A. "Ovidius" *Univ. Ann. Chem.* **2021**, 32, 40-45. DOI: <https://doi.org/10.2478/auoc-2021-0006>.
24. Chahul, H. F.; Maji, E.; Danat, T. B. "Ovidius" *Univ. Ann. Chem.* **2019**, 30, 75-80. DOI: <https://doi.org/10.2478/auoc-2019-0014>.
25. Dahdele, J.; Danaee, I.; Rashed, G. R. *J. Chil. Chem. S.* **2016**, 61, 3025-3030. DOI: <https://doi.org/10.4067/S0717-97072016000300003>.
26. Torres, A. A. A. *J. Appl. Electrochem.* **2007**, 38, 835-841. DOI: <https://doi.org/10.1007/s10800-007-9319-z>.
27. Torres, A. A. A.; González, C. P. Y. *Mater.* **2021**, 14, 1-14. DOI: [10.3390/ma14051316](https://doi.org/10.3390/ma14051316).
28. Oulabbas, A.; Abderrahmane, S. *Mater. Res. Express.* **2019**, 6, 015513. DOI: <https://doi.org/10.1088/2053-1591/aae8b9>.
29. Jessima, M.; Hepziba, S. J.; Rakesh, B. G.; Muthappa, M.; Subhashini, S. *Asian J. Chem.* **2020**, 32, 2055-2060. DOI: <https://doi.org/10.14233/ajchem.2020.22730>.